Essential role for *Ptpn11* in survival of hematopoietic stem and progenitor cells

Gordon Chan,[1,2] *Laurene S. Cheung,[3] *Wentian Yang,[1] Michael Milyavsky,[2,4] Ashley D. Sanders,[2] Shengqing Gu,[2,5] Wan Xing Hong,[3] Aurora X. Liu,[2] Xiaonan Wang,[2,5] Mary Barbara,[6,7] Tarun Sharma,[2] Joehleen Gavin,[3] Jeffery L. Kutok,[8] Norman N. Iscove,[6,7] Kevin M. Shannon,[3] John E. Dick,[2,4] Benjamin G. Neel,[1,2,5] and Benjamin S. Braun[3]

[1]Cancer Biology Program, Beth Israel Deaconess Medical Center and Harvard Medical School, Boston, MA; [2]Campbell Family Cancer Research Institute, Ontario Cancer Institute and Princess Margaret Hospital, University Health Network, Toronto, ON; [3]Department of Pediatrics and the Helen Diller Family Comprehensive Cancer Center, University of California, San Francisco, San Francisco, CA; Departments of [4]Molecular Genetics, [5]Medical Biophysics, and [6]Immunology and [7]McEwen Centre for Regenerative Medicine, University of Toronto, Toronto, ON; and [8]Department of Pathology, Brigham and Women's Hospital, Boston, MA

Src homology 2 domain-containing phosphatase 2 (Shp2), encoded by *Ptpn11*, is a member of the nonreceptor protein-tyrosine phosphatase family, and functions in cell survival, proliferation, migration, and differentiation in many tissues. Here we report that loss of *Ptpn11* in murine hematopoietic cells leads to bone marrow aplasia and lethality. Mutant mice show rapid loss of hematopoietic stem cells (HSCs) and immature progenitors of all hematopoietic lineages in a gene dosage-dependent and cell-autonomous manner. *Ptpn11*-deficient HSCs and progenitors undergo apoptosis concomitant with increased *Noxa* expression. Mutant HSCs/progenitors also show defective Erk and Akt activation in response to stem cell factor and diminished thrombopoietin-evoked Erk activation. Activated *Kras* alleviates the *Ptpn11* requirement for colony formation by progenitors and cytokine/growth factor responsiveness of HSCs, indicating that Ras is functionally downstream of Shp2 in these cells. Thus, Shp2 plays a critical role in controlling the survival and maintenance of HSCs and immature progenitors in vivo. (*Blood*. 2011;117(16):4253-4261)

Introduction

Hematopoiesis is maintained by a small number of multipotent long-term hematopoietic stem cells (LT-HSCs) with extensive self-renewal capability. These cells give rise to lineage-committed progenitors, which produce various types of mature blood cells. Cytokine and growth factor signaling is critical for the sustained production of HSCs and progenitors and directs cellular survival, migration, and differentiation.[1,2]

Src homology 2 (SH2) domain-containing phosphatase 2 (Shp2) is a ubiquitously expressed nonreceptor protein-tyrosine phosphatase (PTP), encoded by the *Ptpn11* gene, which regulates signaling networks and cell fates in many organisms. Shp2 is composed of 2 SH2 domains (N-SH2 and C-SH2), a PTP domain, a C-terminal tail with tyrosyl phosphorylation sites that modulate some RTK signaling pathways, and a proline-rich motif of unknown function. In multiple tissues, Shp2 positively regulates Ras/Erk signaling downstream of receptor tyrosine kinases (RTKs) and cytokine receptors.[3] Shp2 also appears to have cell-type- and/or agonist-dependent effects on the activation of Akt, Jnk, NF-κB, Rho, and Nfat.[3] Germline *PTPN11* mutations underlie approximately 50% of Noonan syndrome, which is characterized by short stature, skeletal abnormalities, cardiac defects, learning disabilities, and a predisposition to hematologic abnormalities, particularly juvenile myelomonocytic leukemia. Somatic gain-of-function mutations in *PTPN11* also are the most common cause of sporadic juvenile myelomonocytic leukemia.[4]

Although Shp2 is required for normal Ras/Erk activation in many contexts,[3] the underlying mechanism shows great diversity and depends on the precise cell type and stimulus involved. Epistasis studies in *Caenorhabditis elegans* and *Drosophila* show that activated *Ras/let-60/ras1* suppresses the effects of *Shp2/ptp-2/csw* loss,[5,6] arguing that Shp2 acts upstream of Ras in these signaling pathways. However, in *C elegans* vulva development and *Drosophila* R7 photoreceptors and muscle precursors, *Shp2/ptp-2/csw* appears to act downstream of *Ras/let-60/ras1* in some contexts.[5,7-9] Furthermore, in the EGL-15/Egfr signaling pathway, *ptp-2* may act parallel to *let-60*.[10] In mice, expression of activated *Kras* ($Kras^{G12D}$) does not completely restore defective lens proliferation and lacrimal gland development caused by the loss of *Ptpn11*.[11] Collectively, these results indicate that Shp2 can act upstream, downstream, or parallel to Ras in different systems, and imply that the consequences and the mediators of Shp2 action must be specifically delineated in particular biologic contexts.

Homozygous inactivation of murine Shp2 results in early embryonic lethality[12-14] because of a critical role of Shp2 in trophoblast stem cell survival.[14] Loss of Shp2 also reduces proliferation and causes aberrant differentiation and death of neural stem and early progenitor cells[15,16]; by contrast, *Ptpn11* deficiency enhances embryonic stem cell self-renewal.[17,18] Studies using in vitro embryonic stem cell differentiation,[18-20] Rag2-deficient blastocyst complementation,[21] embryonic stem cell aggregation,[22] and bone marrow (BM) transplantation[23] assays have suggested a role for Shp2 in promoting mesoderm differentiation and hematopoiesis. However, most of these studies used cells and mice expressing an allele of *Ptpn11* that encodes a truncated Shp2 variant with

Submitted November 15, 2010; accepted February 7, 2011. Prepublished online as *Blood* First Edition paper, February 25, 2011; DOI 10.1182/blood-2010-11-319517.

*L.S.C. and W.Y. contributed equally to this study.

The online version of this article contains a data supplement.

The publication costs of this article were defrayed in part by page charge payment. Therefore, and solely to indicate this fact, this article is hereby marked "advertisement" in accordance with 18 USC section 1734.

increased PTP activity, which could have neomorphic effects in some cell contexts. Furthermore, the role of Shp2 in adult hematopoiesis remains to be established.

Here we show that Shp2 is required for the maintenance of HSCs in a gene dosage-dependent and cell-autonomous manner. We also tested the epistatic relationship of Shp2 and Ras in murine hematopoiesis, and find that constitutive Ras activity suppresses the requirement for Shp2 in myeloid progenitors and HSCs. Together, these data support an essential role of Shp2 upstream of Ras in hematopoietic stem and progenitor cell survival.

Methods

Mice and reconstitution experiments

Ptpn11$^{flox/flox}$ mice were generated previously[24] and were bred to *Mx1-Cre* (The Jackson Laboratory) and *Kras*$^{LSL\text{-}G12D}$ (NCI Mouse Repository) mice, as indicated. To induce *Ptpn11* deletion, newborn *Mx1-Cre;Ptpn11*$^{flox/flox}$ mice were injected intraperitoneally with 3 doses of polyinosinic-polycytidylic acid (pIpC, 150 μg/dose). Control mice were injected in parallel. Mice were monitored and killed at the indicated times or when moribund. For reconstitution experiments, 10^6 BM cells from 6- to 8-week-old *Mx1-Cre;Ptpn11*$^{+/+}$, *Mx1-Cre;Ptpn11*$^{flox/+}$, and *Mx1-Cre;Ptpn11*$^{flox/flox}$ CD45.2$^+$ C57BL/6 mice were injected intravenously, along with 10^5 CD45.1$^+$ wild-type BM cells, into 6- to 8-week-old lethally irradiated (950 cGy) B6.SJL-*Ptprc*^{a} *Pep3*^{b}/BoyJ CD45.1$^+$ recipients. After 5 weeks of engraftment, chimeric mice were treated with 5 doses of pIpC (200 μg/dose). Reconstitution by donor cells was detected by staining peripheral white blood cells with anti-CD45.1 (A20) and anti-CD45.2 (104) antibodies. Mice were maintained in accord with guidelines approved by the animal welfare committees of Harvard Medical School and University Health Network.

Histology and pathology examination

Blood counts were determined using a Hemavet 950FS (Drew Scientific). Tissues and organs were collected in 10% formalin and processed by the Specialized Histopathology Services at Brigham and Women's Hospital in Boston, MA.

Retroviral and lentiviral constructs

To generate pMSCV IRES GFP-Cre (pMIGC), a 1.8-kb fragment containing an EGFP-Cre fusion gene was polymerase chain reaction (PCR)-amplified from plasmid pEGFPCREfrtpgktn5neofrt (a gift of Nigel Killeen, University of California, San Francisco), which contains an NLS-Cre sequence in frame with an N-terminal GFP Cre fusion gene in pEGFP-C1 (Clontech). To create pMIGC, the EGFP-Cre amplicon was subcloned as an *Eco*RI-*Bam*HI fragment into pSP72 (Promega) and then excised as a NcoI-SalI fragment and used to replace the NcoI-SalI GFP segment of pMIG. For Gateway cloning, pMIG-GW and pMIGC-GW were made by inserting the RfA Gateway conversion cassette (Invitrogen) into the unique HpaI cloning site upstream of the IRES sequence in pMIG and pMIGC, respectively. To generate lentivirus expressing the dominant negative p53 mutant GSE56, the truncated NGFR reporter gene was excised from the bidirectional lentiviral construct MA1 and replaced with the GSE56 cDNA.[25] Details of these constructs are available from the authors on request.

Retroviral and lentiviral infection

Retroviral supernatants were derived by transfection of 293T cells at 60% to 80% confluence in 100-mm plates using 30 μL Lipofectamine 2000 (Invitrogen) and 10 μg each of retroviral vector DNA and Ecopac packaging construct (gift of R. Van Etten) combined in a total of 1.5 mL Optimem medium (University of California, San Francisco Cell Culture Facility). Supernatant medium was harvested 48 to 72 hours later and used fresh. Fetal liver cells harvested from E14.5 embryos underwent a 24-hour stimulation period in Stemspan medium (StemCell Technologies) supplemented with 15% fetal calf serum, interleukin-11 100 ng/mL (R&D Systems), FLT3 ligand 50 ng/mL (PeproTech), and stem cell factor (SCF, 100 ng/mL, PeproTech), followed by spin infection at 1000*g* for 1.5 to 2 hours in fresh viral supernatant with polybrene 5 μg/mL. Cells recovered at 37°C for 1 to 3 hours, and the viral supernatant was replaced with stimulation medium. Twenty-four hours later, the spin infection was repeated with fresh virus. The following day, 10 000 green fluorescent protein (GFP)$^+$ cells were sorted directly into 1 mL of methylcellulose medium. For lentiviral infection experiments, lin$^-$ BM cells harvested from control and *Ptpn11*$^{\Delta/\Delta}$ mice 10 days after pIpC induction were incubated with control lentivirus or lentivirus expressing the dominant negative p53 mutant GSE56 at a multiplicity of infection of 50 to 100 for 16 hours. Infected cells were washed and cultured for an additional 48 hours in vitro before staining with the indicated antibodies, and then were sorted as described.

Flow cytometry

Single-cell suspensions of BM, spleen, and peripheral blood were resuspended in phosphate-buffered saline with 2% fetal bovine serum and stained with directly conjugated antibodies specific for c-Kit (2B8), Sca1 (D7), CD127 (A7R34), CD34 (RAM34), CD16/32, (93) and antibodies against lineage (Lin) markers, including CD3 (145–2C11), CD4 (RM4–5), CD8α (53–6.7), CD19 (6D5), CD45/B220 (RA3–6B2), Gr1(Ly-6G), and Ter119. Antibodies were purchased from BD Biosciences PharMingen, eBioscience, or BioLegend. Flow cytometry was performed with an LSRII (BD Biosciences), and data were analyzed with FlowJo software Version 7.5.5 (TreeStar). For cell cycle analyses, cells were stained with Hoechst 33342 (H; Invitrogen) and pyronin Y (PY; Sigma-Aldrich) at 37°C in the presence of verapamil (Sigma-Aldrich), and the mean percentages of cells in G_0 (H^-PY^-), G_1(H^-PY^+), and S/G_2M (H^+PY^+) were quantified by flow cytometry as indicated in the text. To analyze signaling in LK and Lin$^-$Sca1$^+$c-Kit$^+$ (LSK) cells, Lin$^-$ cells were fluorescence-activated cell sorter (FACS)-purified and starved for 1 hour before stimulation with SCF (50 ng/mL) or thrombopoietin (TPO, 50 ng/mL) for 5 or 10 minutes. Cells were fixed with 1.5% paraformaldehyde, permeabilized with acetone, and then stained with anti–c-kit, anti-Sca1, and either anti-pErk or anti-pAkt antibodies, as described previously.[26,27] Phospho-specific antibodies were purchased from Cell Signaling Technology; cytokines were from PeproTech.

Colony assays

Fetal liver cells were harvested, transduced with retrovirus, and subjected to colony (granulocyte-macrophage colony-forming units [CFU-GM]) assays in M3231 methylcellulose (StemCell Technologies) supplemented with granulocyte-macrophage colony-stimulating factor 10 ng/mL (PeproTech). Individual colonies were harvested with a 10-μL pipette under direct microscopic visualization and suspended in 10 μL of water. For genotyping, 4 μL of this suspension was amplified in a multiplex PCR reaction using primers MPC-F (5′-ATGGACGTGGGTGCCTGCAT-3′), MPRC-R (5′-GTCCGCGGTCGCGACGTA-3′), and MPFL-R (5′-CCCAACTAG-CAGCCTGGCAAA-3′) and 35 cycles of 94°C for 30 seconds, 66°C for 90 seconds, and 72°C for 60 seconds. These conditions produce distinct bands for wild-type (81 bp), *flox* (157 bp), and Δ (184 bp) alleles of *Ptpn11*. Detailed PCR conditions are available from the authors on request.

Quantitative reverse-transcribed PCR analysis

Total RNA was isolated from FACS-purified BM populations using the PicoPure Kit (Arcturus Bioscience) and subjected to reverse transcription with SuperScript III First-Strand Synthesis System (Invitrogen). Quantitative PCR assays were performed on an ABI 7500 Fast Real-Time PCR System using the TaqMan Universal PCR master mixture (Applied Biosystems). Predesigned primers and probes used in quantitative PCR assay are listed in supplemental Table 1 (available on the *Blood* Web site; see the Supplemental Materials link at the top of the online article).

Single-cell proliferation assays

SLAM HSCs (Lin$^-$c-kit$^+$Sca1$^+$CD150$^+$CD48$^-$) were FACS-purified and deposited in 60-well Terasaki plates (1 cell/well) in Iscove modified

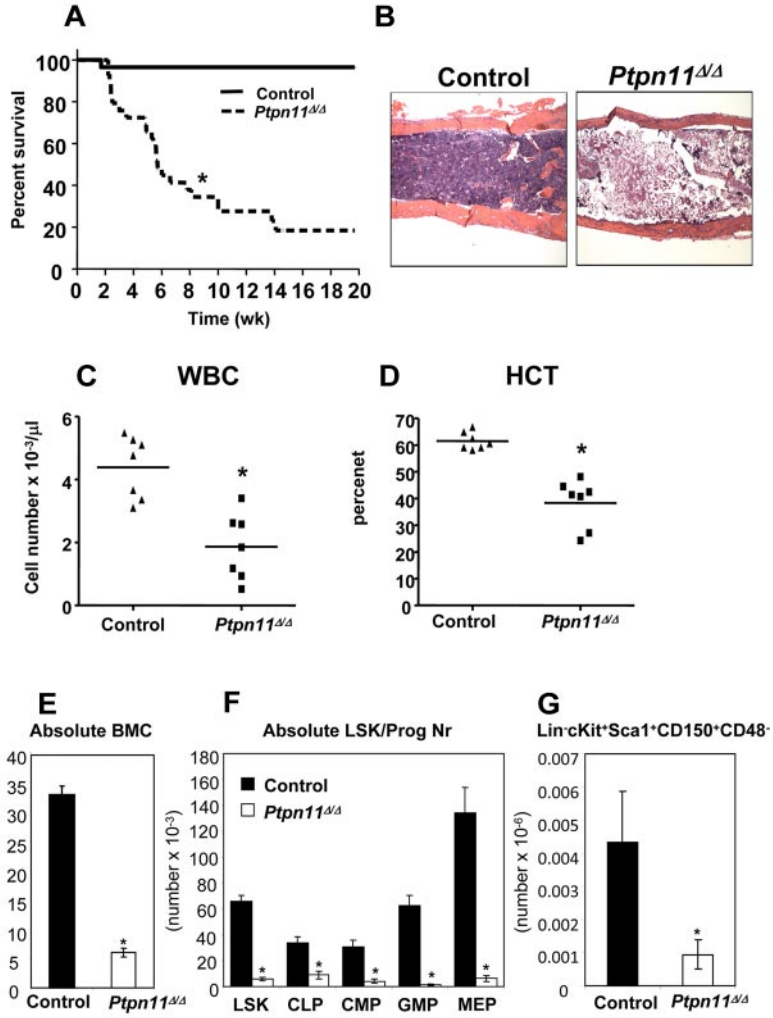

Figure 1. Deletion of *Ptpn11* leads to fatal BM failure and loss of HSCs. (A) Kaplan-Meier survival analysis of a cohort of *Mx1-Cre;Ptpn11*$^{flox/flox}$ (n = 30) and littermate control (n = 28) mice after pIpC treatment. *Ptpn11*$^{\Delta/\Delta}$ mice have a median life span of 5 weeks; control mice remain healthy for > 10 months. *$P < .05$, log-rank test. (B) Hematoxylin and eosin-stained sections from humeri of control and *Ptpn11*$^{\Delta/\Delta}$ animals 4 to 5 weeks after receiving their last dose of pIpC. The samples were analyzed using an Olympus BX41 microscope with the objective lens 4×/0.75 Olympus UPlanFL (Olympus). The pictures were taken using Olympus QColor5 and analyzed with acquisition software QCapture Pro v6.0 (QImaging) and Adobe Photoshop 6.0 (Adobe). (C-D) White blood cell count (WBC; C) and hematocrit (HCT; D) of control and *Ptpn11*$^{\Delta/\Delta}$ mice. *$P < .05$, Student *t* test. (E) BM cellularity (per 2 hind limbs) in control and *Ptpn11*$^{\Delta/\Delta}$ animals shown as mean ± SEM. *$P < .05$, Student *t* test. (F) Absolute number (mean ± SEM). *$P < .05$, Student *t* test. LSK, common lymphoid progenitors (Lin$^-$ Sca1$^+$ c-kit^{lo}IL7Rα^+), common myeloid progenitors (Lin$^-$Sca1$^-$c-kit$^+$CD34$^+$FcγR^{lo}), granulocyte-macrophage progenitors (Lin$^-$Sca1$^-$c-kit$^+$CD34$^+$FcγR^{hi}), megakaryocytic-erythroid progenitors (Lin$^-$Sca1$^-$c-kit$^+$CD34$^-$FcγR$^{-/lo}$) of control (n = 7) and *Ptpn11*$^{\Delta/\Delta}$ mice (n = 7). (G) Absolute number (mean ± SEM). *$P < .05$, Student *t* test. SLAM-HSCs from control (n = 3) and *Ptpn11*$^{\Delta/\Delta}$ mice (n = 3).

Dulbecco medium in the presence of SCF (50 ng/mL), TPO (50 ng/ml), Flt3L (50 ng/mL), interleukin-11 (20 ng/mL), transferrin (5 μg/mL), insulin (5 μg/mL), bovine serum albumin (0.1%), and fetal bovine serum (4%). Cell number in each well was evaluated microscopically on a daily basis for the indicated times.

Statistical analysis

Data are presented as mean ± SEM and analyzed by log-rank test, Student *t* test, or analysis of variance with Bonferroni post-hoc test, as indicated.

Results

Disruption of Shp2 causes BM failure

To begin to assess the role of Shp2 in adult hematopoiesis, we determined its pattern of expression in HSCs and immature hematopoietic progenitors. Quantitative reverse-transcribed PCR analysis (supplemental Figure 1A) revealed similar levels of *Ptpn11* expression in adult LT-HSCs, short-term HSCs, multipotent progenitors, common myeloid progenitors, granulocyte-macrophage progenitors, megakaryocytic-erythroid progenitors, and common lymphoid progenitors. To assess Shp2 function, we bred a conditional mutant (floxed) *Ptpn11* allele[24] onto the *Mx1-Cre* mouse strain, which expresses Cre recombinase (Cre) in response to interferon exposure.[28] *Ptpn11*$^{flox/flox}$ (hereafter, control) and *Mx1-Cre*; *Ptpn11*$^{flox/flox}$ mice were injected with pIpC to induce endogenous interferon production and hence, Cre expression. Most of the induced *Mx1-Cre*; *Ptpn11*$^{flox/flox}$ (hereafter, *Ptpn11*$^{\Delta/\Delta}$) mice became moribund or died by 6 to 8 weeks (Figure 1A). At this time, mutant mice were leukopenic, severely anemic, and had profoundly reduced numbers of BM cells (Figure 1B-E). The remaining surviving *Ptpn11*$^{\Delta/\Delta}$ mice probably have incomplete deletion of the floxed *Ptpn11* allele.

The dramatic phenotype of *Ptpn11*$^{\Delta/\Delta}$ mice led us to examine the HSC-enriched LSK compartment and early progenitors in the mutant BM. Indeed, the frequencies and absolute numbers of LSK, common lymphoid progenitors, common myeloid progenitors, granulocyte-macrophage progenitors, and megakaryocytic-erythroid progenitors were all markedly reduced in *Ptpn11*$^{\Delta/\Delta}$ BM (Figure 1F, supplemental Figure 1B; and data not shown). Analysis of the HSC compartment (LSKCD150$^+$CD48$^-$, also known as SLAM-HSCs) within the LSK population also revealed a marked reduction in cell number, indicating a defect at the earliest stage of adult hematopoietic development (Figure 1G). To assess progenitor cell function, we performed colony assays. Consistent with the flow cytometric data, *Ptpn11*$^{\Delta/\Delta}$ BM cells produced significantly lower numbers of colony-forming units-erythroid, burst-forming units-erythroid, CFU-GM, and colony-forming units granulocyte-erythrocyte-macrophage-megakaryocyte colonies compared with control BM cells (supplemental Figure 1C). Together, these data suggest that the rapid demise of *Ptpn11*$^{\Delta/\Delta}$ mice is probably the

result of severe BM aplasia and the loss of almost all of hematopoietic stem cells and progenitors of the lymphoid, erythroid, and myeloid lineages.

Requirement for Shp2 in HSCs is cell-autonomous

To ask whether the loss of hematopoietic cells in *Ptpn11* mutant animals is cell-autonomous, we transferred uninduced *Mx1-Cre; Ptpn11*$^{+/+}$, *Mx1-Cre;Ptpn11*$^{flox/+}$, and *Mx1-Cre;Ptpn11*$^{flox/flox}$ BM cells expressing the CD45.2 cell surface marker, together with wild-type CD45.1-expressing carrier BM cells, into lethally irradiated congenic CD45.1 animals. Recipients were maintained for 5 weeks to allow sufficient time for steady-state hematopoiesis to be reestablished. Mice were then injected with pIpC, and the ratio of CD45.1$^+$ versus CD45.2$^+$ cells was measured in the peripheral blood. All mice showed comparable levels of CD45.2 engraftment before pIpC treatment. Yet, whereas recipients of *Mx1-Cre; Ptpn11*$^{+/+}$ BM maintained more than 90% CD45.2$^+$ peripheral blood cells for up to 21 weeks after pIpC treatment, the percentage of CD45.2$^+$ cells in peripheral blood was reduced to 50% and 40% in mice that had received *Mx1-Cre;Ptpn11*$^{flox/+}$ and *Mx1-Cre; Ptpn11*$^{flox/flox}$ cells, respectively (Figure 2A). At 21 weeks, donor CD45.2$^+$ cells in recipients of *Mx1-Cre;Ptpn11*$^{flox/+}$ BM cells accounted for 50% of blood neutrophils (Gr1$^+$), 50% of T lymphocytes (CD3$^+$), and 75% of B lymphocytes (B220$^+$) (Figure 2B). By contrast, there was marked attrition of *Mx1-Cre; Ptpn11*$^{flox/flox}$ cells in vivo with 90% of Gr1$^+$ neutrophils, 80% of CD3$^+$ T cells, and 50% of B220$^+$ B cells expressing the recipient CD45.1 marker. Whereas CD45.1$^+$ Lin$^-$c-kit$^+$ competitor cells composed only approximately 20% of BM cells in *Mx1-Cre; Ptpn11*$^{flox/+}$ BM recipients, they represented more than 80% of cells in recipients of *Mx1-Cre;Ptpn11*$^{flox/flox}$ BM. These results indicate that most donor-derived *Mx1-Cre;Ptpn11*$^{flox/flox}$ HSCs were lost by 21 weeks after pIpC induction, as the remaining 40% CD45.2 cells in the peripheral blood were mostly B220$^+$ cells. Interestingly, *CD19-Cre;Ptpn11*$^{flox/flox}$ mice show normal B-cell development and maintenance, suggesting that loss of *Ptpn11* can be tolerated in B-cell lineage (W.Y., L. Pao, and B.G.N., manuscript in preparation).

Induced *Mx1-Cre* mice also show gene deletion in various nonhematopoietic tissues after pIpC treatment. To examine whether loss of *Ptpn11* in these interferon-responsive tissues contributes to the loss of HSCs, we injected wild-type CD45.1$^+$ BM cells into lethally irradiated *Mx1-Cre;Ptpn11*$^{flox/+}$ and *Mx1-Cre;Ptpn11*$^{flox/flox}$ animals. Five weeks after engraftment, the mice were treated with pIpC and peripheral blood cell counts were monitored (Figure 2C). Both *Mx1-Cre;Ptpn11*$^{flox/+}$ and *Mx1-Cre;Ptpn11*$^{flox/flox}$ hosts remained healthy and maintained normal blood counts for more than 21 weeks after pIpC treatment (Figure 2C; and data not shown). Therefore, deletion of *Ptpn11* in nonhematopoietic tissues did not compromise steady-state hematopoiesis of normal BM cells. Together, these data suggest that *Ptpn11* is essential for steady-state hematopoiesis and HSC maintenance in a gene dose-dependent and cell-autonomous manner.

Aberrant cell cycle profile and cell death of *Ptpn11*-deficient HSCs and progenitors

Loss of HSCs and progenitor cells could result from several mechanisms, which include failure to maintain quiescence (loss of self-renewal), decreased proliferation, and/or cell death. We determined the effects of *Ptpn11* deficiency on proliferation by assessing cell-cycle parameters in immature progenitors (lin$^-$c-kit$^+$Sca1$^-$ [LK]) and HSC-enriched LSKCD150$^+$ cells. At early times after

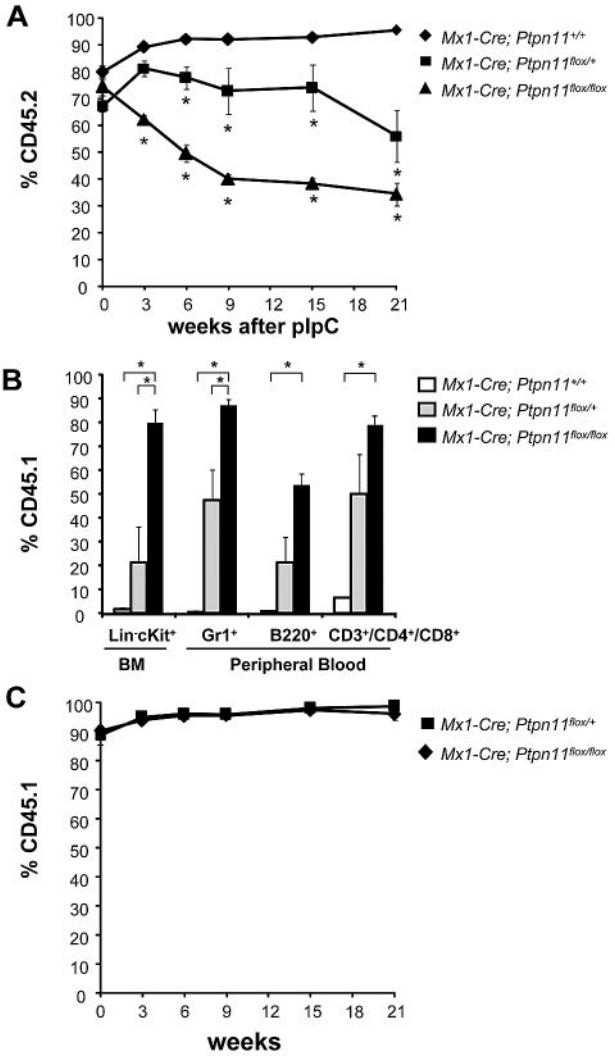

Figure 2. Cell-autonomous requirement for *Ptpn11* in HSC maintenance. (A) Lethally irradiated CD45.1$^+$ recipients were transplanted with 10^6 BM cells from *Mx1-Cre;Ptpn11*$^{+/+}$ (n = 6), *Mx1-Cre;Ptpn11*$^{flox/+}$ (n = 4), or *Mx1-Cre;Ptpn11*$^{flox/flox}$ (n = 4) mice, along with 10^5 wild-type CD45.1$^+$ cells. After 5 weeks of engraftment, chimeric mice were treated with 5 doses of pIpC, and the percentage of peripheral blood cells expressing CD45.1 and CD45.2 was quantified by flow cytometry at the indicated times. *$P < .05$, analysis of variance. (B) Levels of CD45.1$^+$ BM Lin$^-$c-kit$^+$ progenitors (LK) and peripheral blood B220$^+$, CD3$^+$/CD4$^+$/CD8$^+$, and Gr1$^+$ cells were quantified 21 weeks after pIpC induction. *$P < .05$, analysis of variance. (C) Lethally irradiated *Mx1-Cre;Ptpn11*$^{flox/+}$ (n = 4) and *Mx1-Cre;Ptpn11*$^{flox/flox}$ (n = 4) control recipients were transplanted with 10^6 BM cells from wild-type CD45.1$^+$ donors. Mice were treated and analyzed as described in panel A.

pIpC treament, control and *Ptpn11*$^{\Delta/\Delta}$ cells had similar cell cycle profiles. However, compared with controls, *Ptpn11*$^{\Delta/\Delta}$ LK and LSKCD150$^+$ cells consistently exhibited a decreased G_0 population at day 23 after pIpC exposure (Figure 3A-B; supplemental Figure 3). In addition, compared with controls, mutant LSKCD150$^+$ cells showed a significantly higher proportion of cells in G_1. The proportion of mutant LK cells in G_1 also trended higher, although this did not reach statistical significance. *Ptpn11*$^{\Delta/\Delta}$ LK and LSKCD150$^+$ cells also showed significantly increased apoptosis, as revealed by annexin V staining, at 20 and 23 days after pIpC treatment (Figure 3C-D). We also sorted SLAM-HSCs from control and mutant mice 10 days after pIpC induction and placed them at one cell per well in a medium that allows preservation of multipotency in vitro[29] and contains saturating doses of SCF and TPO, 2 cytokines critical for HSC maintenance in vivo.[2] After

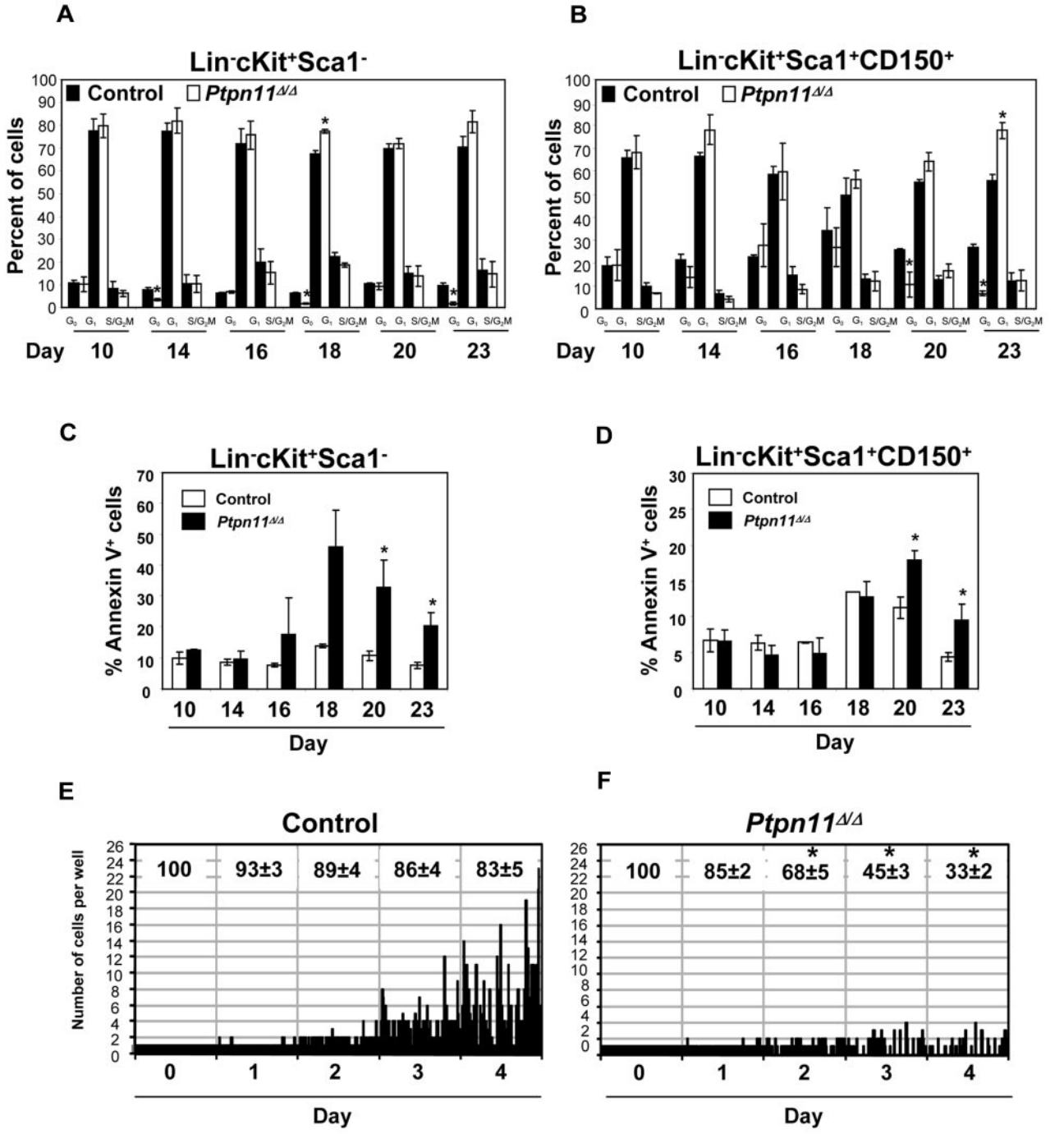

Figure 3. *Ptpn11* deletion leads to decreased quiescence and increased cell death. (A-B) Cell cycle analysis of *Ptpn11*$^{\Delta/\Delta}$ HSCs and progenitors. LK (A) and LSKCD150$^+$ (B) cells were subjected to 2-parameter analysis of DNA content (Hoechst 33342 [H]) vs RNA content (Pyronin [PY]). The mean percentages (± SEM) of cells in G_0 (H^-PY^-), G_1(H^-PY^+), and S/G_2M (H^+PY^+) are indicated. *$P < .05$, Student *t* test. (C) Lin-c-kit$^+$Sca1$^-$ and (D) LSKCD150$^+$ cells harvested from control (n = 3) and *Ptpn11*$^{\Delta/\Delta}$ (n = 3) mice were stained with annexin V to assess cell death at the indicated times after pIpC induction. The average percentage (± SEM) of annexin V$^+$ cells is shown. *$P < .05$, Student *t* test. (E-F) Single SLAM-HSCs were sorted into 60-well plates (1 cell/well) and cultured in media containing SCF, TPO, Flt3L, and interleukin-11. Proliferation of each clone was evaluated microscopically over 4 days. Representative data from one of 4 experiments with similar results are shown. The average percentages (± SEM) of surviving clones from the 4 experiments are shown at the top of each panel. *$P < .05$, Student *t* test.

4 days, more than 80% of control cells were viable and showed substantial proliferation (Figure 3E). By contrast, more than 60% of *Ptpn11*$^{\Delta/\Delta}$ cells had died, whereas the rest had undergone only one or 2 cell divisions (Figure 3F). Together, these data suggest the loss of *Ptpn11* leads to rapid death of HSCs and immature progenitors.

Next, we surveyed the expression of genes previously implicated in the control of cell survival in control and *Ptpn11*$^{\Delta/\Delta}$ LK and HSC-enriched, LSKCD150$^+$ cells. Control and mutant cells expressed similar levels of *Puma*, *Bcl*$_{XL}$, and *Mcl1* (Figure 4A; supplemental Figure 4). Although *Bcl2* expression was comparable in control and *Ptpn11*$^{\Delta/\Delta}$ LSKCD150$^+$ cells, it was down-regulated slightly in *Ptpn11*$^{\Delta/\Delta}$ LK cells; this decrease might contribute to the compromised survival of these cells. More strikingly, however, *Noxa* expression was increased in *Ptpn11*-deficient LK and LSKCD150$^+$ cells, coincident with the onset of cell death. LSK

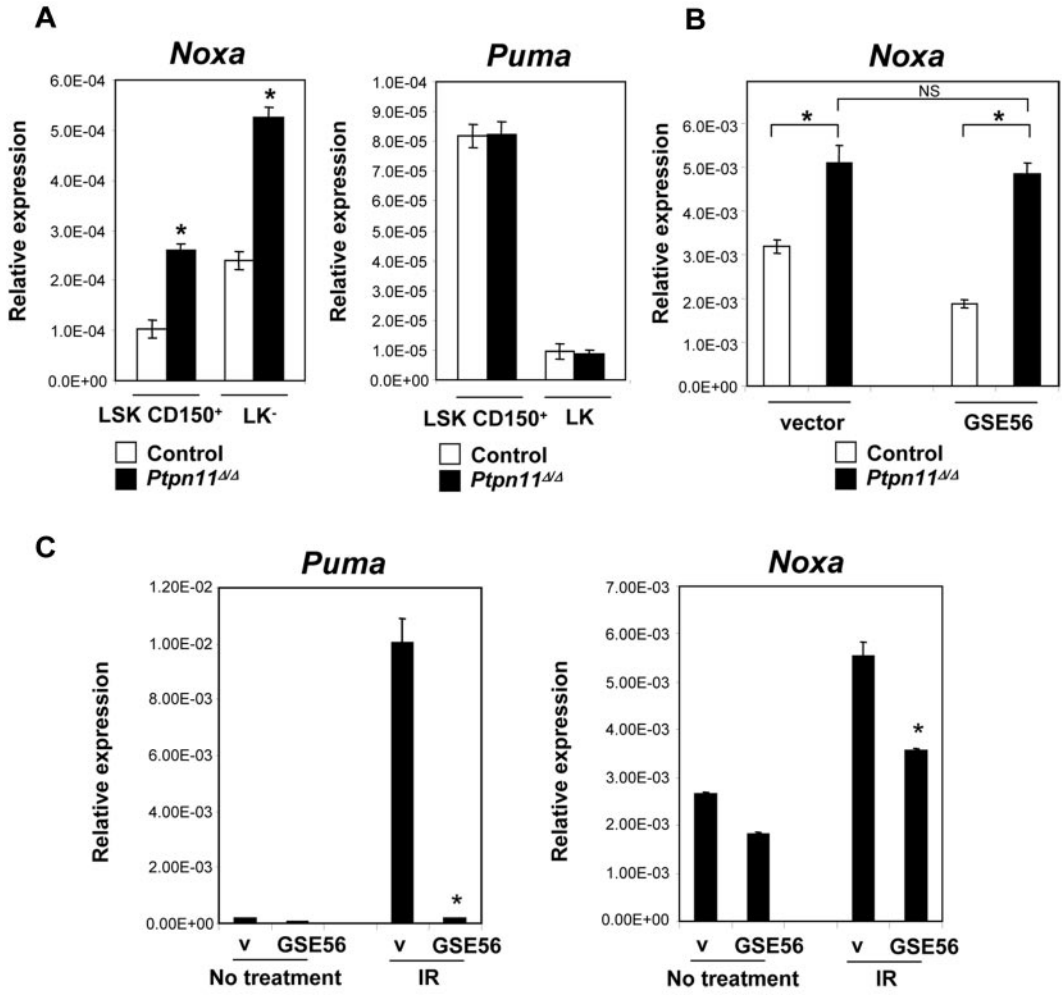

Figure 4. p53-independent up-regulation of *Noxa* in *Ptpn11*$^{\Delta/\Delta}$ HSCs and progenitors. (A) Quantitative PCR of *Noxa* and *Puma* in LSKCD150^{+} and LK cells from control and *Ptpn11*$^{\Delta/\Delta}$ mice 23 days after pIpC induction. Results present mean ± SEM relative to *Gapdh* expression. **P* < .05, Student *t* test. Representative data from one of 4 experiments with similar results are shown. (B) Lin^{-} BM cells, harvested from control and *Ptpn11*$^{\Delta/\Delta}$ mice 10 days after pIpC induction, were infected with control lentivirus or lentivirus expressing a dominant negative p53 mutant (GSE56). Cells were cultured for 48 hours in vitro before staining with anti–c-kit and anti-Sca1 antibodies. GFP^{+} LSK cells were sorted and *Noxa* expression (mean ± SEM) was determined by quantitative PCR. **P* < .05, Student *t* test. NS indicates not significant. Representative data from one of 3 experiments with similar results are shown. (C) Lin^{-} BM cells were infected with control lentivirus or lentivirus expressing GSE56. Cells were cultured for 48 hours in vitro and were left untreated or irradiated (IR, 300 cGy), harvested, and subjected to quantitative PCR as described in panel B. The levels of *Puma* and *Noxa* normalized to *Gapdh* expression are shown (mean ± SEM). **P* < .05, Student *t* test.

cells harvested from control and *Ptpn11* mutant mice 10 days after pIpC treatment showed no signs of apoptosis (Figure 3D) or elevated *Noxa* expression (data not shown); however, on in vitro culture for 48 hours, mutant cells showed significant cell death (Figure 3F; and data not shown) and markedly elevated *Noxa* levels (Figure 4B).

Because *Noxa* can be regulated by p53,[30] and Shp2 inhibits p53-dependent apoptosis in neural crest-derived cells,[31] we asked whether cell death in *Ptpn11*$^{\Delta/\Delta}$ hematopoietic progenitor cells was p53-dependent. Immunoblots of lin^{-}c-kit^{+} BM cells from control and *Ptpn11*$^{\Delta/\Delta}$ mice showed that p53 was not present at a detectable level (data not shown). Furthermore, overexpressing GSE56, a dominant negative mutant of p53,[25] in mutant LSK cells failed to rescue their proliferative response to SCF and TPO (supplemental Figure 5) and did not prevent elevated expression of *Noxa* (Figure 4B). By contrast, GSE56 expression in wild-type lin^{-} BM cells completely blocked the *Puma* and *Noxa* up-regulation in response to irradiation (Figure 4C), indicating that GSE56 was expressed at a level sufficient to block p53 activity in these cells. Together, these data strongly suggest that apoptosis induced by *Ptpn11* deficiency in HSCs/progenitors is p53-independent.

Perturbed SCF and TPO signaling in *Ptpn11*$^{\Delta/\Delta}$ stem/progenitor cells

The failure of *Ptpn11*$^{\Delta/\Delta}$ HSCs to expand in response to cytokine and growth factor stimulation led us to interrogate signaling pathways downstream of key receptors, such as Kit and Mpl, in these cells. Multiparameter flow cytometric analysis showed that SCF-evoked Erk and Akt activation was reduced substantially in *Ptpn11*$^{\Delta/\Delta}$ LSK and LK cells (Figure 5A,C). Although TPO-evoked Akt activation was unaffected by *Ptpn11* deficiency (Figure 5D), TPO-evoked Erk activation was markedly reduced in *Ptpn11*$^{\Delta/\Delta}$ LSK cells (Figure 5B). STAT3 and STAT5 activation were similar in control and and *Ptpn11* mutant cells, and there was no detectable activation of Erk or Akt in response to TPO in either control or mutant LK cells (data not shown). Notably, control and *Ptpn11*-deficient LK and LSK cells express similar levels of *Mpl* RNA (supplemental Figure 6). Together, these data demonstrate that mutant LSK and LK cells show

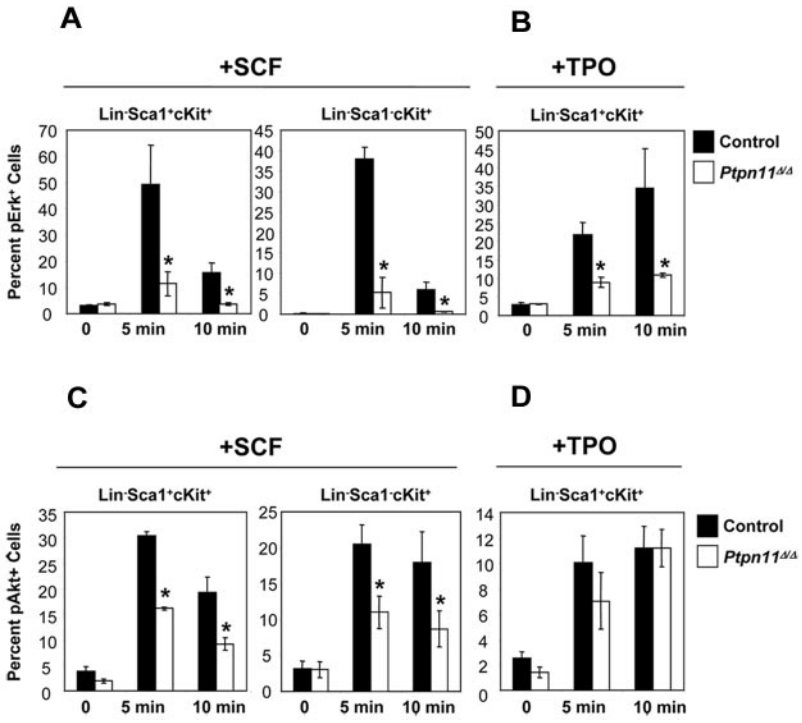

Figure 5. Signaling defects in *Ptpn11*$^{\Delta/\Delta}$ LSK and LK cells. Lin$^-$ BM cells from control (n = 4) and *Ptpn11*$^{\Delta/\Delta}$ (n = 4) mice were purified by FACS and starved for 1 hour in serum-free media, before they were either left untreated or stimulated with SCF (50 ng/mL) or TPO (50 ng/mL) for the indicated times. Cells were fixed, permeabilized, and stained with anti–c-kit, anti-Sca1, and anti-pErk (A-B) or pAkt (C-D). Levels of phospho-specific antigens in the LSK and LK population were determined by flow cytometry. The percentages of pErk$^+$ or pAkt$^+$ cells from 4 experiments are shown as mean ± SEM. *$P < .05$, Student *t* test.

compromised growth factor and cytokine receptor signaling, which probably accounts for their impaired proliferation and survival in vitro and in vivo.

Kras activation is epistatic to *Ptpn11* disruption in HSCs and myeloid progenitors

We tested whether Ras activation is the required signal downstream of Shp2 in HSCs/progenitors by asking whether a gain-of-function *Ras* allele could suppress the effects of *Ptpn11* deletion. Embryonic day 14.5 fetal liver cells were transduced with retroviral vectors expressing GFP or a GFP-Cre fusion protein. GFP$^+$ cells were isolated by FACS and plated in methylcellulose containing granulocyte-macrophage colony-stimulating factor (Figure 6A). We observed nearly complete loss of CFU-GM in *Ptpn11*$^{flox/flox}$ cells expressing GFP-Cre and the hygromycin resistance gene. Colony growth was rescued by coexpression of *Ptpn11* cDNA, indicating

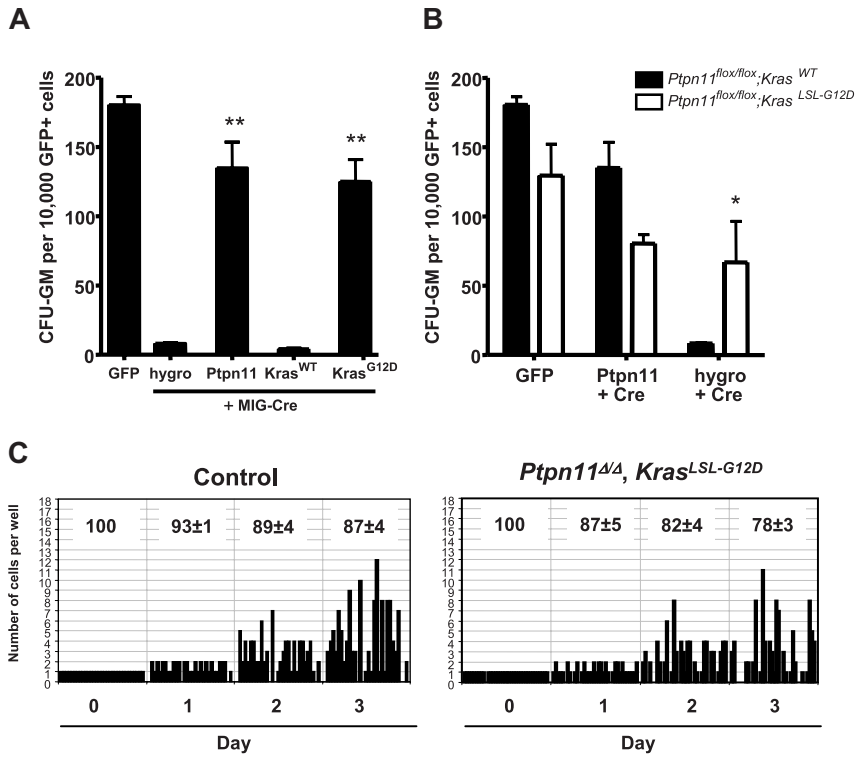

Figure 6. Expression of activated *Kras* compensates for loss of *Ptpn11* in HSCs and progenitors. (A) Primary myeloid progenitors from embryonic day 14.5 *Ptpn11*$^{flox/flox}$ fetal livers were transduced with the indicated retroviruses, and FACS-purified GFP$^+$ cells were cultured in methylcellulose medium containing granulocyte-macrophage colony-stimulating factor. GFP virus served as a negative control. MIG-Cre vectors were designed to coexpress the hygromycin resistance gene, WT *Ptpn11*, WT *Kras*, or activated *Kras*^{G12D}. Results are shown as mean ± SEM of 3 independent experiments. *$P < .05$, Student *t* test. **$P < .01$, Student *t* test. (B) Effect of *Ptpn11* loss in *Ptpn11*$^{flox/flox}$ fetal liver cells with or without an activated *Kras*$^{LSL-G12D}$ allele. Cells of the indicated genotype were transduced with GFP virus control or with MIG-Cre virus coexpressing exogenous *Ptpn11* or the hygromycin resistance gene. Results are shown as mean ± SEM of 3 independent experiments. *$P < .05$, Student *t* test. (C) SLAM-HSCs from control (n = 2) and *Mx1-Cre*; *Kras*$^{LSL-G12D}$; *Ptpn11*$^{flox/flox}$ (n = 4) mice were purified by FACS and deposited into 60-well plates (1 cell/well), and proliferation of each clone was evaluated microscopically over 3 days. The average percentages (± SEM) of surviving clones are shown at the top of each panel. Representative data from these experiments with similar results are shown.

that the lack of colony formation was the result of the loss of *Ptpn11*. These data indicate that, in addition to its role in adult hematopoiesis, Shp2 also is required for the survival and/or growth of fetal liver myeloid progenitors. To test the ability of activated Ras to rescue this phenotype, we constructed a vector coexpressing GFP-Cre and a constitutively active isoform of *Kras*. *Ptpn11*$^{flox/flox}$ cells expressing GFP-Cre and the oncogenic *Kras*^{G12D} allele were able to form CFU-GM. Importantly, these cells showed complete deletion of *Ptpn11* (supplemental Figure 7A). These data demonstrate that overexpression of activated *Kras* can alleviate the requirement for *Ptpn11* in fetal liver myeloid progenitors.

Next, we asked whether *Ptpn11*-deficient CFU-GM could be rescued by activated *Kras* expressed at normal levels, using fetal liver cells from *Ptpn11*$^{flox/flox}$ mice that also contained the *Kras*$^{LSL\text{-}G12D}$ conditional knock-in allele. In these cells, Cre expression simultaneously causes deletion of *Ptpn11* and expression of activated *Kras*^{G12D} under the control of its endogenous promoter. *Ptpn11*$^{flox/flox}$; *Kras*$^{LSL\text{-}G12D}$ fetal liver cells transduced with the *hygro* GFP-Cre vector formed robust colonies, whereas cells lacking the *Kras*$^{LSL\text{-}G12D}$ allele could not (Figure 6B). PCR analysis of individual colonies verified the *Kras*^{G12D} *Ptpn11*$^{\Delta/\Delta}$ genotype (supplemental Figure 7B). These results confirm that constitutive K-Ras activation overcomes the requirement for Shp2 in myeloid progenitors.

Finally, we asked whether *Kras*^{G12D} expression could rescue the growth factor/cytokine proliferation of adult *Ptpn11*-deficient HSCs. SLAM-HSCs were harvested from control and *Mx1-Cre*; *Ptpn11*$^{flox/flox}$ *Kras*$^{LSL\text{-}G12D}$ mice and subjected to single-cell proliferation assays. As shown in Figure 6C, the number of mutant clones that proliferated was similar to that of control cells. Analysis by quantitative PCR indicated complete absence of *Ptpn11* mRNA in LK mutant cells (supplemental Figure 7C). Together, these data demonstrate that hyperactive Ras is epistatic to Shp2 loss in primary hematopoietic stem and progenitor cells, consistent with a model in which Ras activation is a major function provided by Shp2 in these cells.

Discussion

Genetic data that directly address the role of the Ras/Erk pathway in HSCs function are limited. In this report, we identify a cell-autonomous requirement for Shp2 in the survival and maintenance of HSCs and immature hematopoietic progenitors in vivo. A previous study showed that mice with heterozygous expression of a *Ptpn11* truncation allele have normal BM cellularity and peripheral blood counts but impaired HSC function.[23] Our data reveal a much more profound requirement for Shp2, as complete absence of both *Ptpn11* alleles leads to rapid and severe attrition of the hematopoietic system. Because differentiated B cells and macrophages are largely unaffected in CD19 Cre;*Ptpn11*$^{flox/flox}$ (W.Y., L. Pao, and B.G.N., manuscript in preparation) and LysM Cre;*Ptpn11*$^{flox/flox}$ mice, respectively (W.Y. and B.G.N, manuscript in revision), our data further suggest that the loss of these lineages in pIpC-treated Mx*Cre*; *Ptpn11*$^{flox/flox}$ mice is largely the result of depletion of immature progenitors and/or HSCs.

Loss of *Ptpn11*-deficient LSKCD150^{+} and LK populations is accompanied by apoptosis (Figure 3C-D) and a reduction of G_0 cells, concomitant with accumulation of G_1 cells (Figure 3A-B). The latter might reflect impaired G_1/S progression in the absence of *Ptpn11*. However, as the aberrant cell cycle profile only becomes evident 23 days after pIpC treatment, it probably reflects an attempt of mutant HSCs/progenitors to respond to the rapid depletion of mature BM cells in *Ptpn11*$^{\Delta/\Delta}$ mice. *Ptpn11*-deficient HSCs also could be prone to enter the cell cycle because of defective Tpo/Mpl signaling (Figure 5), which is crucial for maintaining quiescence of postnatal HSCs.[32,33] Together, our data show that the loss of *Ptpn11*-mutant HSCs and progenitor cells is accompanied by the loss of quiescence and increased cell death.

Death of *Ptpn11* mutant hematopoietic progenitor cells is detectable only 20 days after pIpC treatment, whereas the absolute number of mutant progenitors begins to decline by day 14 (data not shown). Yet, complete absence of *Ptpn11* mRNA was observed by day 10 (supplemental Figure 2; and data not shown), and LSK cells harvested at this time show defective Erk activation after SCF stimulation, consistent with the complete absence of Shp2 protein as well. A possible explanation for the lag between loss of *Ptpn11* expression and the onset of apoptosis is that dead cells are phagocytosed rapidly by myeloid cells, so that increased apoptosis cannot be detected at early times after *Ptpn11* deletion. As *Ptpn11*-deficient myeloid progenitors and mature myeloid cells are progressively depleted, apoptotic cells accumulate. Consistent with this notion, *Ptpn11*$^{\Delta/\Delta}$ SLAM-HSCs harvested at day 10 after pIpC treatment undergo rapid cell death in vitro (Figure 3E-F) when they are cultured in a cytokine cocktail that preserves WT HSC multipotency in vitro.[29]

Noxa expression is markedly up-regulated in *Ptpn11*-deficient HSC-enriched LSKCD150^{+} cells and immature hematopoietic progenitors, correlating with the onset of apoptosis in these cells. *Noxa* is a transcriptional target of p53,[30,34] and Shp2 can suppress p53-dependent apoptosis.[31] Surprisingly, however, *Noxa* up-regulation and death of *Ptpn11*$^{\Delta/\Delta}$ immature hematopoietic progenitors are p53-independent. Shp2 also is known to suppress p73-dependent apoptosis,[35] but *p73* was not expressed at detectable levels in control or *Ptpn11* mutant HSCs and progenitors (data not shown). Interestingly, *Noxa* is up-regulated in a p53-independent manner in T cells after CD3 stimulation and helps limit T-cell survival.[36,37] Increased *Noxa* levels in *Ptpn11*$^{\Delta/\Delta}$ cells might promote cell death by antagonizing Mcl1, which is critical for HSC survival.[30,37,38] Genetic experiments to address the requirement of *Noxa* and the role of Mcl1 in triggering apoptosis in *Ptpn11*-deficient HSCs and progenitors are ongoing.

In conclusion, we find that endogenous expression of a constitutively active *Kras* allele rescues *Ptpn11*$^{\Delta/\Delta}$ HSCs and myeloid progenitor cells in vivo, placing Ras downstream of or parallel to Shp2 in a pathway controlling hematopoietic stem and progenitor cell survival. Thus, hematopoietic progenitors behave similarly to *C elegans* oocytes or *Drosophila melanogaster* embryos, in which activated Ras alleles suppress Shp2 deficiency ("Introduction"). By contrast, activated K-Ras does not fully rescue *Ptpn11* deficiency in lens and lacrimal gland development,[11] a finding attributed to the loss of Shp2-mediated antagonism of Sprouty2 (a negative regulator of the Ras/Erk pathway). Our data suggest that Sprouty-independent regulation of Ras signaling is more dominant in murine HSCs and progenitors. Together, our observations are consistent with the genetics of juvenile myelomonocytic leukemia and Noonan syndrome,[4] which place mutant *PTPN11* in the *RAS* signaling pathway. Our data show that introducing *Kras*^{G12D} can suppress the requirement for *Ptpn11* in HSCs and immature progenitors. It is not clear whether this reflects a specific requirement for K-Ras and whether N-Ras or H-Ras would have similar effects. Future experiments will also establish which pathways downstream of *Kras*^{G12D} are required to suppress the *Ptpn11*$^{\Delta/\Delta}$ phenotype. Such studies might inform therapeutic approaches and minimize hematologic side effects in treating patients with somatic or germline mutant *PTPN11*.

Acknowledgments

The authors thank Pier-André Pentillä for expert assistance with flow cytometry and David Tuveson and Tyler Jacks for providing *LSL-Kras*^{G12D} mice.

This work was supported by the National Institutes of Health (grant RO1 CA114945, B.G.N.; grant R01 CA104282, K.M.S.; and in part, grant P20 RR025179, W.Y.), the Ontario Ministry of Health and Long Term Care, Concern Foundation, and the American Society of Hematology (Scholar award; B.S.B.).

The views expressed do not necessarily reflect those of the Ontario Ministry of Health and Long Term Care.

Authorship

Contribution: G.C. and B.S.B. designed and performed research, analyzed data, and wrote the paper; L.S.C., W.Y., M.M., A.D.S., S.G., W.X.H., A.X.L., X.W., M.B., T.S., J.G., and J.L.K. performed research and analyzed data; N.N.I. and J.E.D. analyzed data; K.M.S. designed research and analyzed data; and B.G.N. designed research, analyzed data, and wrote the paper.

Conflict-of-interest disclosure: The authors declare no competing financial interests.

The current affiliation of W.Y. is Department of Orthopaedics, and COBRE Center for Stem Cell Biology, Brown University Alpert Medical School, and Rhode Island Hospital, Providence, RI.

Correspondence: Gordon Chan, Campbell Family Cancer Research Institute, Ontario Cancer Institute, 101 College St, TMDT Rm 8-301, Toronto, ON M5G 1L7, Canada; e-mail: gordon.chan@uhnresearch.ca; and Benjamin G. Neel, Campbell Family Cancer Research Institute, Ontario Cancer Institute, 101 College St, TMDT Rm 8-301, Toronto, ON M5G 1L7, Canada; e-mail: bneel@uhnresearch.ca.

References

1. Orkin SH, Zon LI. Hematopoiesis: an evolving paradigm for stem cell biology. *Cell.* 2008;132(4):631-644.
2. Zhang CC, Lodish HF. Cytokines regulating hematopoietic stem cell function. *Curr Opin Hematol.* 2008;15(4):307-311.
3. Neel BG, Chan G, Dhanji S. SH2 domain-containing protein-tyrosine phosphatases. In: *Handbook of Cell Signaling*, 2nd ed. Oxford, United Kingdom: Academic Press; 2009:771-810.
4. Tartaglia M, Gelb BD. Noonan syndrome and related disorders: genetics and pathogenesis. *Annu Rev Genomics Hum Genet.* 2005;6:45-68.
5. Gutch MJ, Flint AJ, Keller J, Tonks NK, Hengartner MO. The Caenorhabditis elegans SH2 domain-containing protein tyrosine phosphatase PTP-2 participates in signal transduction during oogenesis and vulval development. *Genes Dev.* 1998;12(4):571-585.
6. Lu X, Chou TB, Williams NG, Roberts T, Perrimon N. Control of cell fate determination by p21ras/Ras1, an essential component of torso signaling in Drosophila. *Genes Dev.* 1993;7(4):621-632.
7. Hopper NA. The adaptor protein soc-1/Gab1 modifies growth factor receptor output in Caenorhabditis elegans. *Genetics.* 2006;173(1):163-175.
8. Allard JD, Chang HC, Herbst R, McNeill H, Simon MA. The SH2-containing tyrosine phosphatase corkscrew is required during signaling by sevenless, Ras1 and Raf. *Development.* 1996;122(4):1137-1146.
9. Johnson Hamlet MR, Perkins LA. Analysis of corkscrew signaling in the Drosophila epidermal growth factor receptor pathway during myogenesis. *Genetics.* 2001;159(3):1073-1087.
10. Schutzman JL, Borland CZ, Newman JC, Robinson MK, Kokel M, Stern MJ. The Caenorhabditis elegans EGL-15 signaling pathway implicates a DOS-like multisubstrate adaptor protein in fibroblast growth factor signal transduction. *Mol Cell Biol.* 2001;21(23):8104-8116.
11. Pan Y, Carbe C, Powers A, Feng GS, Zhang X. Sprouty2-modulated Kras signaling rescues Shp2 deficiency during lens and lacrimal gland development. *Development.* 2010;137(7):1085-1093.
12. Saxton TM, Henkemeyer M, Gasca S, et al. Abnormal mesoderm patterning in mouse embryos mutant for the SH2 tyrosine phosphatase Shp-2. *EMBO J.* 1997;16(9):2352-2364.
13. Arrandale JM, Gore-Willse A, Rocks S, et al. Insulin signaling in mice expressing reduced levels of Syp. *J Biol Chem.* 1996;271(35):21353-21358.
14. Yang W, Klaman LD, Chen B, et al. An Shp2/SFK/Ras/Erk signaling pathway controls trophoblast stem cell survival. *Dev Cell.* 2006;10(3):317-327.
15. Ke Y, Zhang EE, Hagihara K, et al. Deletion of Shp2 in the brain leads to defective proliferation and differentiation in neural stem cells and early postnatal lethality. *Mol Cell Biol.* 2007;27(19):6706-6717.
16. Gauthier AS, Furstoss O, Araki T, et al. Control of CNS cell-fate decisions by SHP-2 and its dysregulation in Noonan syndrome. *Neuron.* 2007;54(2):245-262.
17. Burdon T, Stracey C, Chambers I, Nichols J, Smith A. Suppression of SHP-2 and ERK signalling promotes self-renewal of mouse embryonic stem cells. *Dev Biol.* 1999;210(1):30-43.
18. Qu CK, Shi ZQ, Shen R, Tsai FY, Orkin SH, Feng GS. A deletion mutation in the SH2-N domain of Shp-2 severely suppresses hematopoietic cell development. *Mol Cell Biol.* 1997;17(9):5499-5507.
19. Zou GM, Chan RJ, Shelley WC, Yoder MC. Reduction of Shp-2 expression by small interfering RNA reduces murine embryonic stem cell-derived in vitro hematopoietic differentiation. *Stem Cells.* 2006;24(3):587-594.
20. Chan RJ, Johnson SA, Li Y, Yoder MC, Feng GS. A definitive role of Shp-2 tyrosine phosphatase in mediating embryonic stem cell differentiation and hematopoiesis. *Blood.* 2003;102(6):2074-2080.
21. Qu CK, Nguyen S, Chen J, Feng GS. Requirement of Shp-2 tyrosine phosphatase in lymphoid and hematopoietic cell development. *Blood.* 2001;97(4):911-914.
22. Qu CK, Yu WM, Azzarelli B, Cooper S, Broxmeyer HE, Feng GS. Biased suppression of hematopoiesis and multiple developmental defects in chimeric mice containing Shp-2 mutant cells. *Mol Cell Biol.* 1998;18(10):6075-6082.
23. Chan RJ, Li Y, Hass MN, et al. Shp-2 heterozygous hematopoietic stem cells have deficient repopulating ability due to diminished self-renewal. *Exp Hematol.* 2006;34(9):1230-1239.
24. Zhang SQ, Yang W, Kontaridis MI, et al. Shp2 regulates SRC family kinase activity and Ras/Erk activation by controlling Csk recruitment. *Mol Cell.* 2004;13(3):341-355.
25. Ossovskaya VS, Mazo IA, Chernov MV, et al. Use of genetic suppressor elements to dissect distinct biological effects of separate p53 domains. *Proc Natl Acad Sci U S A.* 1996;93(19):10309-10314.
26. Kalaitzidis D, Neel BG. Flow-cytometric phosphoprotein analysis reveals agonist and temporal differences in responses of murine hematopoietic stem/progenitor cells. *PLoS One.* 2008;3(11):e3776.
27. Chan G, Kalaitzidis D, Usenko T, et al. Leukemogenic Ptpn11 causes fatal myeloproliferative disorder via cell-autonomous effects on multiple stages of hematopoiesis. *Blood.* 2009;113(18):4414-4424.
28. Kuhn R, Schwenk F, Aguet M, Rajewsky K. Inducible gene targeting in mice. *Science.* 1995;269(5229):1427-1429.
29. Benveniste P, Cantin C, Hyam D, Iscove NN. Hematopoietic stem cells engraft in mice with absolute efficiency. *Nat Immunol.* 2003;4(7):708-713.
30. Ploner C, Kofler R, Villunger A. Noxa: at the tip of the balance between life and death. *Oncogene.* 2008;27(suppl 1):S84-S92.
31. Stewart RA, Sanda T, Widlund HR, et al. Phosphatase-dependent and -independent functions of Shp2 in neural crest cells underlie LEOPARD syndrome pathogenesis. *Dev Cell.* 2010;18(5):750-762.
32. Qian H, Buza-Vidas N, Hyland CD, et al. Critical role of thrombopoietin in maintaining adult quiescent hematopoietic stem cells. *Cell Stem Cell.* 2007;1(6):671-684.
33. Yoshihara H, Arai F, Hosokawa K, et al. Thrombopoietin/MPL signaling regulates hematopoietic stem cell quiescence and interaction with the osteoblastic niche. *Cell Stem Cell.* 2007;1(6):685-697.
34. Oda E, Ohki R, Murasawa H, et al. Noxa, a BH3-only member of the Bcl-2 family and candidate mediator of p53-induced apoptosis. *Science.* 2000;288(5468):1053-1058.
35. Amin AR, Thakur VS, Paul RK, et al. SHP-2 tyrosine phosphatase inhibits p73-dependent apoptosis and expression of a subset of p53 target genes induced by EGCG. *Proc Natl Acad Sci U S A.* 2007;104(13):5419-5424.
36. Alves NL, Derks IA, Berk E, Spijker R, van Lier RA, Eldering E. The Noxa/Mcl-1 axis regulates susceptibility to apoptosis under glucose limitation in dividing T cells. *Immunity.* 2006;24(6):703-716.
37. Wensveen FM, van Gisbergen KP, Derks IA, et al. Apoptosis threshold set by Noxa and Mcl-1 after T cell activation regulates competitive selection of high-affinity clones. *Immunity.* 2010;32(6):754-765.
38. Opferman JT, Iwasaki H, Ong CC, et al. Obligate role of anti-apoptotic MCL-1 in the survival of hematopoietic stem cells. *Science.* 2005;307(5712):1101-1104.